

Yacora on the Web: Online Collisional Radiative Models for plasmas containing H, H₂ or He

D. Wunderlich¹, M. Giacomini², R. Ritz³, and U. Fantz¹

¹: Max-Planck-Institut für Plasmaphysik, 85748 Garching, Germany

²: École Polytechnique Fédérale de Lausanne, 1015 Lausanne, Switzerland

³: Max Planck Computing and Data Facility, 85748 Garching, Germany

Abstract

Yacora on the Web (www.yacora.de) is a web application providing access to collisional radiative models based on the flexible solver Yacora. The main application range is plasma diagnostics in low-pressure plasmas. Available online are three collisional radiative models, namely for atomic hydrogen, molecular hydrogen and helium. This paper gives a brief overview to collisional radiative modeling and to the Yacora solver. The functionality of Yacora on the Web is introduced and the three available models as well as the used input data are presented and discussed. As application example, the models for atomic and molecular hydrogen are applied for investigating spontaneous emission in ionizing and recombining plasmas. This application shows a very good agreement between measured and calculated emission intensities as well as between plasma parameters from other diagnostics and those derived using Yacora on the Web from optical emission spectroscopy results.

Introduction

Population models predict population densities of excited states in atoms, molecules (or atomic or molecular ions) and their dependence on plasma parameters as the electron temperature T_e and the electron density n_e . Additional important input parameters can be the quasi-constant densities of the ground states of one or more particle species, the temperatures of such particle species as well as the population densities of metastable excited states.

Backward application of population models can be used for plasma diagnostics. For example, by matching calculated population densities to results of optical emission spectroscopy (OES) the plasma parameters can be determined [1]. Forward application of population models enable predicting for known plasma parameters the population densities of excited states. The latter can be useful, for example, for predicting the photon emission of atomic lines as well as molecular bands, and consequently e.g. photon fluxes towards surfaces [2].

The kind of population model providing the most broad application range (between very low and very high electron densities) are Collisional Radiative (CR) models. Usually, this type of model is applied to plasmas with a collision rate too high for corona models and too low for the (local) thermodynamic equilibrium (LTE). However, CR models intrinsically include the corona model and for high collision rates their results should converge to the population distributions predicted by the LTE.

Yacora [3] is a solver for coupled sets of ordinary differential equations with focus on the application for rate equations used in plasma physics. Yacora can be used for constructing CR models but also other types of models based on rate equations like dissociation models. The solver supports the definition of reaction probabilities (both for electron collisions and heavy particle collisions) via rate coefficients or cross sections. When using the latter, arbitrary energy probability functions (EPF) can be used for the electrons while for all heavy particle species a Maxwell distribution function is applied. CR models based on Yacora are available for a set of atomic and molecular species, with focus on application in low-pressure plasmas (up to several Pa). In these plasmas electron collision reactions are dominant. For higher pressures heavy particle collisions not implemented in the current models can play a significant role for the steady-state population of the excited states [4].

The aim of this paper is to introduce Yacora on the Web, a web framework making available to the public CR models based on Yacora. First, an overview of CR modeling in general, the Yacora solver and the available models is given. Then, the Yacora on the Web framework is described and finally examples for the application of Yacora on the Web are given.

Collisional Radiative modelling

CR models predict in a wide parameter range the population densities of excited states in atoms, molecules or the respective ions. For each excited state included into the model all relevant excitation and de-excitation processes are balanced in a zero-dimensional approximation. Equation 1 shows, as example, the rate equation for the population density n_p of the excited state p in an atom:

$$\frac{dn_p}{dt} = \sum_{q>p} A_{qp}n_q - \sum_{q<p} A_{pq}n_p + n_e \left(\sum_{q \neq p} X_{qp}n_q - \sum_{q \neq p} X_{pq}n_p + (\alpha + \beta n_e)n_+ - S_p n_p \right), \quad (1)$$

where A_{qp} and A_{pq} are the transition probabilities for spontaneous emission from q to p and p to q , respectively. X_{qp} and X_{pq} are the rate coefficients for excitation or de-excitation by electron collisions and n_e the electron density. α and β are the rate coefficients for radiative and three-body recombination of a positive ion with density n_+ and S_p is the rate coefficient for ionization of the state p . Equation 1 must be extended when additionally other processes have to be considered. Examples for such processes are: excitation or de-excitation by collisions with particles other than electrons, the transport of metastable states via diffusion (the probability of this process can be approximated in zero-dimensional models by effective lifetimes [5]) and self-absorption caused by optical thickness [6].

The rate equations for all excited states included into the CR model form a set of coupled ordinary differential equations (ODE). Different methods exist for solving this set of ODE. The simplest one is inverting a matrix, see for example [7]. This procedure intrinsically only works for linear problems, as in Equation 1, where only electron collisions, spontaneous emission and radiative recombination play a role and the plasma is optically thin.

Another method is integrating the differential equations, starting with appropriate initial conditions, typically defined as input parameter by the user of the model. Performing an integration has the

disadvantage to be computationally more expensive than a simple matrix inversion. However, non-linear processes (examples are optical thickness and collisions between two excited atoms or molecules) can be implemented in a self-consistent manner. This results in a significant extension of the application range. For example, collisions between excited states can be of high relevance in equilibrium plasmas and/or high (atmospheric) pressure plasmas. Integrating the differential equations additionally allows for investigating the temporal evolution of the population densities after changes in the plasma parameters.

The intensity ε_{pq} of an emission line $p \rightarrow q$ can be deduced from the population density n_p of the excited state p by multiplication with the respective transition probability A_{pq} :

$$\varepsilon_{pq} = A_{pq}n_p. \quad (2)$$

When solving CR models, usually the fact is exploited that the (population) densities of some particle species or excited states can be in quasi-steady-state, i.e. they change on a much slower time scale than the other excited states. Examples are the ground state of the atom or the molecule itself and its ions as well as metastable states. The (population) densities of these particles or states can be treated as fixed and used as initial conditions for the set of ODE to be solved. They can be determined by using codes (for example dissociation models or transport codes) or simple assumptions (e.g. n_e is equal to the sum of the positive and negative ion densities or the density of a neutral particle follows the ideal gas law).

For constructing CR models for atoms, the probabilities of up to several thousand reactions interconnecting the excited states implemented into the model have to be known in form of cross sections, rate coefficients or transition probabilities. The complexity increases dramatically for molecules where vibrational and rotational excitation results in a huge increase of the number of excited states. When the probability for a certain reaction is not known, it can be deduced by assumptions or extrapolations, e.g. from the known probability of a similar reaction, but this procedure includes the risk of significant uncertainties. The uncertainty of reaction probabilities can be directly correlated to the uncertainty of the model results. Consequently, an important step in developing CR models is the validation of the implemented reaction probabilities. This is particularly important if for specific reactions different data sets exist with significant differences in the given reaction probabilities, as it is the case for electron collision excitation of the hydrogen molecule [8].

Yacora and Yacora on the Web

Yacora integrates systems of rate equations (for example Equation 1) with the aim of obtaining the steady-state population densities of excited atomic or molecular states. Yacora on the Web uses an upper integration limit of 20 s; this is by several orders of magnitude higher than what is needed for establishing the steady-state.

The typical time scales of different reaction types in a plasma can strongly differ. For example, for $T_e=3$ eV and $n_e=10^{17} \text{ m}^{-3}$ the reaction rate for spontaneous emission $n=3 \rightarrow n=2$ in the hydrogen atom is $\approx 8 \text{ s}^{-1}$ per atom in the ground state, compared to $\approx 5 \cdot 10^{-3} \text{ s}^{-1}$ for collisional de-excitation, i.e. spontaneous emission is by a factor of more than 1000 faster than collisional de-excitation. This means that the set of differential equations is stiff and integrators based on the Euler or Runge Kutta procedure (the used time step is

defined by the typical time scale of the fastest reaction) can consume a very high amount of computational time. In order to keep the computational time within reasonable limits, Yacora is based on the CVODE [9] solver for stiff sets of differential equations. CVODE is part of the SUNDIALS package developed at the Lawrence Livermore National Laboratory (LLNL). The CVODE solver for stiff sets of ordinary differential equations is based on Backwards Differentiation Formulas (BDFs). The typical calculation time for a single calculation, i.e. determining for one combination of plasma parameters the steady-state population density of the excited states in an atom or molecule, is below 1 s.

Available for Yacora are a multitude of extensively validated and benchmarked CR models for different atomic and molecular species (see for example [8, 10]; some of the molecular models include the vibrational or the ro-vibrational sub-levels). These models have been applied for plasma diagnostics at numerous experiments worldwide (see, for example, [11, 12, 13, 14, 15, 16, 17, 18]), with focus on low-pressure plasmas. The steadily increasing interest triggered the development of Yacora on the Web, a web application, providing access to the Yacora CR models for atomic and molecular hydrogen and for helium. These models have been chosen since they are amongst the most thoroughly benchmarked Yacora CR models.

Yacora on the Web runs on a virtual Linux machine and is based on the Plone 5 framework [19]. The communication between Plone and Yacora itself is realized via a set of Python scripts. The system allows users to perform a simple self-registration. An extensive documentation on the implemented CR models is available. Figure 1 shows the login screen of Yacora on the Web. Each user has its own home folder where the input parameter and the results for all calculations performed by the user are stored.

The following steps summarize the workflow of Yacora on the Web:

1. A user selects one of the three available CR models (H, H₂, He) and submits a set of input parameters.
2. A reviewer checks the coherence of the submitted input parameters and starts the calculation. Aim of the coherence check is to identify in advance combinations of input parameters that are physically meaningless and/or would result in a too long calculation time.
3. After the calculation is performed, the results are stored in the user's home folder and the user is informed via e-mail.

If an error occurs during the calculation process, both the reviewer and the user are informed via e-mail.

The Yacora models for H, H₂ and He

Helium and atomic as well as molecular hydrogen are present in different kinds of plasmas, ranging from astrophysics to plasma-processing devices and fusion experiments. CR models for atomic hydrogen and helium are under development since many decades: The first CR model for H was developed by Johnson and

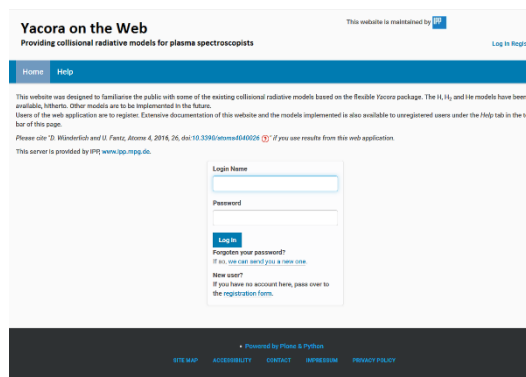


Figure 1: Log in screen of Yacora on the Web.

Hinnov [20] and since then other CR models for the hydrogen atom have been presented [21, 22]. The same holds for helium atom: the development of CR models started early [23] and a multitude of models are available now [24, 25, 26, 27]. Despite the higher complexity, also several different CR models for H_2 are available [28, 29, 30, 31, 32]. Given here is a short introduction into the CR models for these species available via Yacora on the Web. A more detailed overview can be found elsewhere [8].

The CR model for helium comprises all excited states with principal quantum number $p \leq 4$ and the singly ionized positive ion. The electron excitation cross-sections are taken from [33, 34], and the probabilities for spontaneous emission from [35]. De-excitation cross-sections are calculated by the detailed balance principle [36]. Two different procedures are available for defining the population densities of the metastable states 2^1S and 2^3S : first, these population densities can be fixed to values defined by the user of the model, i.e. the metastable states are treated as equivalent to additional ground states. Second, the model can approximate the transport of the metastable states by diffusion using the diffusion cross section for helium atoms in a helium background [37]. The probability for diffusion is defined via characteristic lengths of the plasma. In cases where a full description of the diffusion process is not possible (due to the 0D character of the model or due to processes not implemented to the model like photo-absorption), these characteristic lengths can be used as fitting parameters.

The model for H includes all excited states with $p \leq 40$, including the transition to the ionic continuum, and the positive ion. The reason for implementing – compared to the model for He – excited states up to a much higher quantum number is that this is necessary for ensuring a correct description of the population densities for states with quantum numbers up to $p=10 \dots 20$. Recombining processes can strongly increase the population densities of these states and spontaneous emission originating from these states can be easily detectable in recombining plasmas. Consequently, they can be relevant for plasma diagnostic, see e.g. [12]. The cross sections for electron collision excitation are from [38, 39]. These have been used for determining rate coefficients based on Maxwell electron EPF and the correction for electron energies close to the threshold described in [3] have been applied. De-excitation cross sections are calculated by the detailed balance. Besides direct excitation (from the atomic ground state) other excitation channels involving particle species with quasi-constant densities are included; the cross sections for these processes are taken from: recombination of H^+ [28], dissociative excitation of H_2 [28], dissociative recombination of H_2^+ [39], dissociative recombination of H_3^+ [40, 41], mutual neutralization of H^- with positive ions [39, 42]. Probabilities for spontaneous emission are taken from [43, 44].

The model for the hydrogen molecule includes all electronic states of the singlet and triplet systems up to the principal quantum number $p=10$. Ro-vibrational splitting of the states is neglected. For the states with $p \leq 3$ the splitting due to the angular momentum of the electrons is implemented. This is of high relevance for plasma diagnostics since the transitions originating from these states can be clearly distinguished in measured emission spectra. Cross sections for electron collision excitation from the ground state to the excited states with $p=2$ and $p=3$ in both multiplet systems have been taken from [39] or [45]; the web application allows to switch between the data from the one reference to the other one. For excitation of states with higher principal quantum numbers, cross sections from [28] are used. The Gryzinski method [46, 47] was used to calculate cross sections for electron collision processes between electronically excited states. Spin exchange collisions between excited states are neglected. Transition probabilities for

spontaneous emission have been taken from [28]. Additionally included to the model are the following loss channels for excited molecular states: de-excitation (quenching) of the states c^3 and a^3 by collisions with the background gas, charge exchange of H^+ with excited states of H_2 and dissociative attachment of electrons to excited states of H_2 . The reaction probabilities for the latter three processes are taken from [48], [29, 49] and [50], respectively. These reactions can be switched on and off by the user of Yacora on the Web.

Although in principle the impact of optical thickness on the population density of excited states can easily be added to Yacora models, the three CR models available via Yacora on the Web do not include it. The reason is that the population escape factors [6] needed for implementing optical thickness strongly depend on the geometry of the plasma source and parameters like the gas temperature. Calculating these factors is very time consuming and cannot be done on the fly. If for any of the Yacora on the Web models optical thickness needs to be taken into account, it is recommended to modify the model results taking into account the individual plasma specifications. For example, the correction factors described in [6] can be applied in order to assess the enhancement of excited state population densities caused by optical thickness. These factors depend on the ground state density and on the gas temperature (the latter affecting the profile of the emitting line). Assessing the accuracy of this method is not straight-forward but it can be stated that even small deviations in the mentioned physical parameters can have a large effect on the predicted population densities.

Besides the impact of self-absorption on the population densities of excited states and consequently the number of emitted photons, additionally the loss of photons during their transport through the plasma (described by line escape factors [51]) may play a role.

Application of Yacora on the Web

Presented in this section are results of applying Yacora on the Web to emission of the hydrogen atom and molecule, measured in ionizing and recombining plasmas within RF driven negative hydrogen ion source test facilities for neutral beam heating (NBI) at the international fusion experiment ITER. A comprehensive overview of these ion sources and their application can be found elsewhere [52, 53].

In one or more cylindrical RF drivers a low-pressure, low-temperature hydrogen or deuterium plasma is generated by inductive coupling ($f=1$ MHz, P_{RF} up to 100 kW). The filling pressure is 0.3...0.6 Pa. Negative ions are generated by the surface process [54], mainly by conversion of hydrogen atoms [55] on the caesiated low work function surface of the plasma grid, the first grid of a multi-aperture, multi-grid extraction and acceleration system.

While expanding towards the plasma grid, both the electron temperature and density in the driver plasma ($T_e \approx 10$ eV and $n_e \approx 10^{18} \text{ m}^{-3}$ [56]) are reduced by about one order of magnitude by means of a magnetic filter field [57]. This reduction results in an effectively increased characteristic length of negative ion destruction by electron collisions (from well below one millimeter in the driver to several tens of centimeters at the plasma grid [58]) and consequently a high (up to ≈ 30 %) extraction probability for negative ions generated at the plasma grid surface [59].

The driver plasma is ionizing [60]. The most relevant excitation channel for atomic hydrogen emission is direct electron collision excitation from the atomic ground state. Molecular radiation is more or less exclusively caused by direct excitation of H_2 . The plasma close to the extraction system is recombining [60]: atomic radiation is caused by recombining processes, mainly dissociative recombination of molecular ions and mutual neutralization of negative ions with positive ions.

Figure 2 shows a sketch of the RF driven prototype ion source used at the BATMAN Upgrade test facility [52, 61]. Indicated are the RF driver, the plasma grid and typical lines of sight (LOS) used for OES measurements in the driver and the recombining plasma close to the extraction system. Application of OES as plasma diagnostic in such ion sources is described in [1, 62, 63, 64].

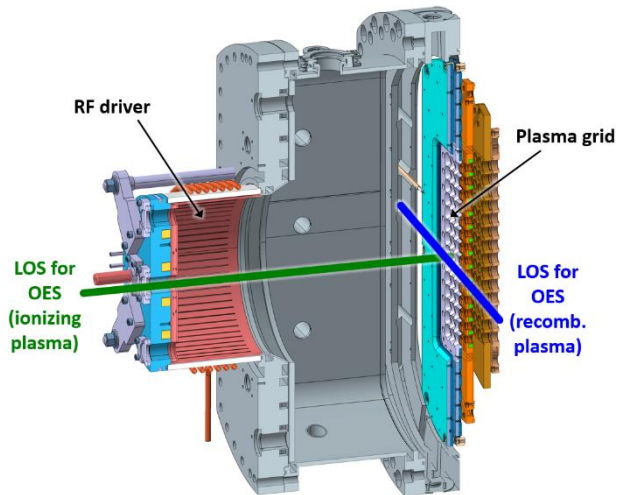


Figure 2: Sketch of the RF driven prototype ion source for ITER NBI. Indicated are the RF driver, the plasma grid and two LOS used for OES measurements of the ionizing driver plasma and the recombining plasma of the expansion region.

Knowledge of the plasma parameters in both regions – as can be gained by application of CR models to photon emission measured by OES – is crucial for an effective source operation and for optimizing source parameters as for example the strength of the filter field. In both cases, ionizing and recombining plasmas, the emission is correlated to the temperatures and densities of all particle species involved in the excitation process.

Given in the following as example for the application of Yacora on the Web are evaluations of OES results from both the driver plasma and the plasma close to the plasma grid.

Ionizing plasma

One of the most relevant plasma parameters in the negative hydrogen ion sources for ITER NBI is the atomic hydrogen flux onto the plasma grid surface, determining the amount of negative ions produced at the grid surface.

Dissociation of hydrogen molecules into atoms predominately takes place in the driver(s). The ratio of atomic to molecular density in the driver(s) can be treated as a measure for the atomic flux onto the plasma grid. In order to determine this ratio, usually the line ratio method proposed in [62, 63, 65] is applied. This method is based on the emission of the atomic Balmer line H_ν ($n=5 \rightarrow 2$) and the molecular Fulcher band ($d^3 \rightarrow a^3$), measured by OES. The evaluation typically is based on CR model calculations, assuming only excitation from the respective ground state in both the atom and the molecule.

Applied here is a more comprehensive evaluation method, based on fitting results of Yacora on the Web to measured emission of the first four Balmer lines H_α to H_δ ($n=3..6 \rightarrow 2$) and the Fulcher band. The ion source was operated at an RF power of 70 kW and a filling pressure of 0.3 Pa.

Yacora on the Web was applied for calculating population densities of the excited states in the hydrogen atom and the hydrogen molecule. These calculations were done for a wide range of electron temperatures (150 interpolation values between 8 eV and 20 eV) and electron densities (150 interpolation values between 10^{17} m^{-3} and 10^{19} m^{-3}), i.e. around the parameters expected for the driver [56]. The calculations for the atomic hydrogen were done for all direct, dissociative and recombining excitation channels included to the model. The calculation for H_2 was done using the set of input cross sections from [39]. Switched on were the three optional loss channels quenching of c^3 and a^3 , charge exchange of H^+ with H_2 and dissociative attachment of electrons to H_2 . The results of the model for H have been corrected for the impact of self-absorption of the resonant Lyman lines on the population densities of the upper states of the Balmer lines [6].

The fit procedure was invoked for each possible combination of the interpolation values for electron temperature and electron density (i.e. 22500 times). For each step, the atomic and molecular emission calculated by using equation 2 was adjusted to results from OES applied to the driver plasma of BATMAN Upgrade. Free parameters are the densities of the species involved in the different direct, dissociative and recombining excitation channels (H , H^+ , H_2 , H_2^+ , H_3^+ and H^-). Used as starting values and as boundary conditions for these parameters are physically reasonable estimations (e.g. the sum of the positive and negative ion densities has to be equal the electron density, the neutral particle densities should not be too far away from the ideal gas law and the ionization and dissociation degree not too far from measurement results [62] achieved for comparable plasmas).

If for a specific type of plasma the plasma parameters can be determined by separately evaluating measured line intensities, then also the described fitting routine should yield reliable results. This is the case for the examples given in this paper. For the ionizing plasma the fitting procedure, combining the intensities of several Balmer lines and the molecular Fulcher band with the described boundary conditions enabled finding a reasonable small solution set, i.e. combination of T_e and n_e for that a good match between the measured and calculated line and band emission can be achieved. The best match between the Balmer and Fulcher emission calculated for these densities and the measured emission has been determined using the least squares method.

Figure 3 shows the measured atomic and molecular emission together with the results of the performed fit. A very good agreement between measurement and the Yacora on the Web results is found. The blue curves indicate the share of the

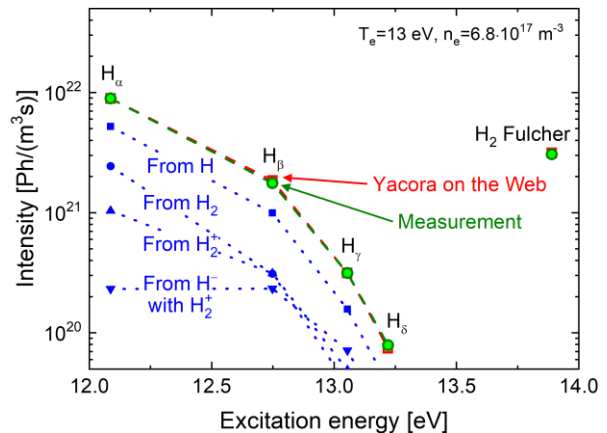


Figure 3: Balmer line and Fulcher band emission measured in the driver of the NBI test facility BATMAN Upgrade for an RF power of 70 kW and a filling pressure of 0.3 Pa. Absolute emission predicted by Yacora on the Web for $T_e=13 \text{ eV}$ and $n_e=6.7 \cdot 10^{17} \text{ m}^{-3}$. Share of the Balmer line emission resulting from different excitation channels. The dashed and dotted lines act as a guide for the eye only.

Balmer emission related to direct excitation of H, dissociative excitation of H₂, dissociative recombination of H₂⁺ and mutual neutralization of H⁻ with H₂⁺. As expected, direct excitation is the by far most relevant process. Although the densities of H⁻ and H₂⁺ determined by the fit are small (about one and two orders of magnitude smaller than the atomic density, respectively), a high reaction probability causes a non-negligible fraction of excitation caused by mutual neutralization.

The densities of atomic and molecular hydrogen have been determined to $4.3 \cdot 10^{18} \text{ m}^{-3}$ and $3.1 \cdot 10^{19} \text{ m}^{-3}$, representing a ratio of atomic to molecular density of 14 %. The electron density is $6.8 \cdot 10^{17} \text{ m}^{-3}$ and the electron temperature 13 eV. While the electron density can be determined with an acceptable error bar ($\pm 2.5 \cdot 10^{17} \text{ m}^{-3}$), the uncertainty in the electron temperature is high (several eV) in this parameter range, caused by the fact that for electron temperatures above ≈ 10 eV the excitation rate coefficients depend only weakly on T_e.

This high uncertainty in the electron temperature demonstrates that fitting CR model results to experimental data can result in ambiguous results. This is caused – besides the abovementioned weak dependence of the model results on the plasma parameters in some parameter ranges – by the strongly multidimensional character of the problem. In order to avoid misleading results, it is strongly suggested to critically check the results of such fitting procedures, especially, when they are used for automatically determining plasma parameters. Such check could be based, for example, on a comparison of the model results with known plasma parameters for similar plasmas.

The plasma parameters determined for the ionizing plasma are in good agreement to results of Langmuir probe measurements done for similar plasma parameters [56]. For these plasma parameters, optical thickness of the Lyman lines results in an increase of the Balmer emission between ≈ 29 % (for H_α) and ≈ 4 % (for H_γ).

Applying to the measured data the line ratio method instead of the performed fitting procedure, i.e. using only the radiation of H_γ and of the Fulcher band as well as assuming direct excitation only, results in a ratio of atomic to molecular density of 29 %, which is significantly higher than the result of the fitting procedure. The reason for this discrepancy is that when neglecting in the evaluation the other excitation channels besides direct excitation, the share of Balmer radiation originating from H₂, H₂⁺ and H⁻ has to be substituted by an increased density of hydrogen atoms. Consequently, when interpreting Balmer lines measured in plasmas where these other excitation channels are not completely negligible, the line ratio method can be applied only for a rough estimation of the plasma parameters. For decreasing the uncertainty of the results either the line ratio method has to be extended taking into account all relevant excitation channels [65]. Alternatively, a full evaluation (using the absolute intensity of the transitions instead of the line ratios) can be applied, for example based on Yacora on the Web.

Recombining plasma

In order to minimize the destruction of negative ions by collisions with electrons [57], electron temperatures below 2 eV together with reduced electron densities (by one order of magnitude compared to the 10^{18} m^{-3} present in the driver [57]) are envisaged for negative hydrogen ion sources for ITER NBI. The presence of such low electron temperatures and densities have been demonstrated by means of

Langmuir probes [66] in the prototype source with a magnetic filter generated solely by permanent magnets.

At the large (size of the ion source: 1×1 m) RF driven ELISE test facility [52], the main component of the filter field is generated by a current, I_{PG} , flowing in vertical direction through the plasma grid. The field strength resulting from this current can be continuously adjusted, up to ≈ 5 mT close to the plasma grid (for $I_{PG}=5.3$ kA). One important task of plasma diagnostics during the early operation of ELISE was to check if the I_{PG} magnetic filter causes a sufficient reduction in T_e and n_e .

The emission of the Balmer lines H_α , H_β and H_γ ($n=3\dots 5 \rightarrow 2$) was measured by OES in the plasma close to the plasma grid (the used LOS is parallel to the plasma grid and has a distance of 2 cm). The source was operated at an RF power of 20 kW/driver and a filling pressure of 0.7 Pa.

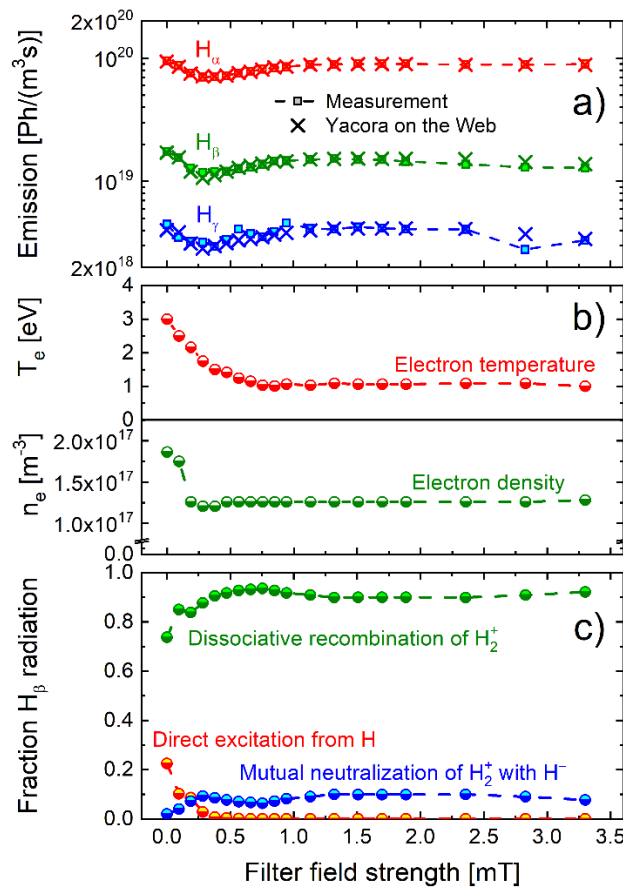


Figure 4: Yacora on the Web results for the recombining plasma close to the plasma grid of the NBI test facility ELISE using an RF power of 20 kW/driver and a filling pressure of 0.7 Pa. a) comparison of measured and calculated Balmer line emission versus the filter field strength. b) Electron temperature and electron density. c) relative relevance of the different excitation channels.

operated at an RF power of 20 kW/driver and a filling pressure of 0.7 Pa.

Due to the high number of (potentially) relevant excitation channels in recombining plasmas, the line ratio method is not applicable. Thus, again a fitting procedure has been applied and as prerequisite for this fitting procedure, Yacora on the Web was applied for calculating population densities of the excited states of H for all excitation channels. These calculations were done for a wide range of electron temperatures (150 interpolation values between 0.1 eV and 5 eV) and electron densities (75 interpolation values between 10^{16} m^{-3} and 10^{18} m^{-3}), again including the parameters expected for the plasma under investigation. Again, the influence of optical thickness of the Lyman lines on the Balmer line radiation is taken into account by scaling the Yacora on the Web results.

Figure 4a) shows the measured Balmer line emission versus the strength of the magnetic filter together with the results of the fit procedure based on Yacora on the Web. Over the whole range of the filter field strength the agreement is very good. The atomic hydrogen density was adjusted by the fit routine to values between 1.8 - and $3 \cdot 10^{18}$ m^{-3} . For these values of $n(H)$, optical thickness results in an increase of the Balmer emission between ≈ 60 % (for H_α) and ≈ 9 % (for H_γ).

Figure 4b) shows T_e and n_e determined by the fit: with increasing filter field strength, the electron temperature and density drop from ≈ 3 eV and $\approx 2 \cdot 10^{17} \text{ m}^{-3}$ to about 1 eV and $1.2 \cdot 10^{17} \text{ m}^{-3}$, respectively.

The reduction of T_e to 1 eV is accompanied with an increase of the negative ion density from $\approx 10^{15} \text{ m}^{-3}$ to $\approx 5 \cdot 10^{15} \text{ m}^{-3}$, in good agreement with measurements in other ion sources [67]. These results demonstrate that magnetic filters based on a current flowing through the plasma grid can fulfill their purpose in large negative ion sources.

Figure 4c) shows the share of the H_β emission caused by three different excitation channels. Without filter field the plasma is partly ionizing: besides dissociative recombination of H_2^+ and mutual neutralization of H_2^+ and H^- also direct excitation of hydrogen atoms is partially responsible ($\approx 20\%$) for the H_β emission. With increasing filter field strength, the relevance of the direct excitation decreases, mainly caused by the reduction in T_e , until for filter field strengths above 0.25 mT the plasma is fully recombining. For this strength of the filter, the electrons start being magnetized (the Larmor radius reaches ≈ 1 cm) while the field strength is too low over the whole scan for magnetizing the ions. With further increasing field strength, the ratio of the two recombinative excitation channels slightly varies. A probable explanation is a slight modification of the plasma parameters induced by a vertical plasma drift observed in the experiment [52]. This plasma drift is caused by the interplay of the filter field with electrostatic fields and pressure gradients (diamagnetic drift) [68, 69]. However, for all values of the filter field strength dissociative recombination of H_2^+ is the by far most relevant excitation channel for excited atomic states.

Conclusions

Collisional radiative models for H, H_2 and He based on the flexible solver Yacora are now available via the web application Yacora on the Web. Yacora on the Web allows an easy self-registration process and provides an extensive documentation of the implemented models. Diffusion of the metastable states of He is implemented by means of effective lifetimes. The models do not include the effect of optical thickness on the population of excited states; it has to be determined individually (taking into account the geometry and the parameters of the specific plasma) by scaling the model results. Presented as examples are the application of the models for H and H_2 to ionizing and recombining plasmas in RF driven negative hydrogen ion sources. While in the ionizing case the plasma parameters derived from the results of Yacora on the Web agree well with Langmuir probe results, the parameters determined for the recombining case proved the functionality of the magnetic filter of the negative ion test facility ELISE. After the successful launch of Yacora on the Web, the next step will be the extension by other particle species. Potential candidates are neutral argon and its positive ion. Also possible is the extension of the parameter range to which the models can be applied towards high (atmospheric) pressure plasmas. The latter extension would make Yacora on the Web available to a multitude of plasma experiments like for example plasma jets or plasma torches.

References

- [1] FANTZ, U.; Basics of plasma spectroscopy, **Plasma Sources Sci. Technol.** **15**, 2006, S137.
- [2] FANTZ, U.; BRIEFI, S.; RAUNER, D.; WÜNDERLICH, D.; Quantification of the VUV radiation in low pressure hydrogen and nitrogen plasmas, **Plasma Sources Sci. Technol.** **25**, 2016, 045006.
- [3] WÜNDERLICH, D.; DIETRICH, S.; FANTZ, U.; Application of a collisional radiative model to atomic hydrogen for diagnostic purposes, **J. Quant. Spectrosc. Radiat. Transfer** **110**, 2009, 62.
- [4] BACRI, J.; GOMES, A.M.; Influence of atom-atom collisions on thermal equilibrium in argon arc discharges at atmospheric pressure, **J. Phys. D** **11**, 1978, 2185.
- [5] MÖLLER, W.; Plasma and surface modeling of the deposition of hydrogenated carbon films from low-pressure methane plasmas, **Appl. Phys. A** **56**, 1993, 527.
- [6] BEHRINGER, K.; FANTZ, U.; The influence of opacity on hydrogen excited-state population and applications to low-temperature plasmas, **New J. Phys.** **2**, 2000, 23.
- [7] PERT, G.J.; Models of collisional-radiative recombination, **J. Phys. B** **23**, 1990, 619.
- [8] WÜNDERLICH, D.; FANTZ, U.; Evaluation of State-Resolved Reaction Probabilities and Their Application in Population Models for He, H, and H₂, **Atoms** **4**, 2016, 26.
- [9] HINDMARSH, A.C.; BROWN, P.N.; GRANT, K.E.; LEE, S.L.; SERBAN, R.; SHUMAKER, D.E.; WOODWARD, C.S.; SUNDIALS: Suite of Nonlinear and Differential/Algebraic Equation Solvers, **ACM Trans. Math. Softw.** **31**, 2005, 363.
- [10] FANTZ, U.; WÜNDERLICH, D.; Atomic and Molecular Collisional Radiative Modeling for Spectroscopy of Low Temperature and Magnetic Fusion Plasmas, **AIP Conf. Proc.** **1344**, 2011, 204.
- [11] FRIEDL, R.; FANTZ, U.; Spectral intensity of the N₂ emission in argon low-pressure arc discharges for lighting purposes, **New J. Phys.** **14**, 2012, 043016.
- [12] POSPIESZCZYK, A.; REINHART, M.; UNTERBERG, B.; BREZINSEK, S.; KRETER, A.; SAMM, U.; SERGIENKO, G.; SCHWEER, B.; SALMAGNE, C.; REITER, D. et al.; Spectroscopic characterisation of the PSI-2 plasma in the ionising and recombining state, **J. Nucl. Mater.** **438**, 2013, S1249.
- [13] BARBISAN, M.; BALDADOR, C.; ZANIOL, B.; CAVENAGO, M.; FANTZ, U.; PASQUALOTTO, R.; SERIANNI, G.; VIALETTO, L.; WÜNDERLICH, D.; First hydrogen operation of NIO1: Characterization of the source plasma by means of an optical emission spectroscopy diagnostic, **Rev. Sci. Instrum.** **87**, 2016, 02B319.

- [14] BRIEFI, S.; GUTMANN, P.; RAUNER, D.; FANTZ, U.; Comparison of the B field dependency of plasma parameters of a weakly magnetized inductive and Helicon hydrogen discharge, **Plasma Sources Sci. Technol.** **25**, 2016, 035015.
- [15] FRIEDL, R.; KURUTZ, U.; FANTZ, U.; Efficiency of Cs-free materials for negative ion production in H₂ and D₂ plasmas, **AIP Conf. Proc.** **1869**, 2017, 030022.
- [16] MARINI, C.; AGNELLO, R.; DUVAL, B.P.; FURNO, I.; HOWLING, A.A.; JACQUIER, R.; KARPUSHOV, A.N.; PLYUSHCHEV, G.; VERHAEGH, K.; GUITTIENNE, Ph. et al.; Spectroscopic characterization of H₂ and D₂ helicon plasmas generated by a resonant antenna for neutral beam applications in fusion, **Nucl. Fusion** **57**, 2017, 036024.
- [17] NISHIDA, K.; MATTEI, S.; BRIEFI, S.; BUTTERWORTH, A.; GRUDIEV, A.; HAASE, M.; JONES, A.; PAOLUZZI, M.M.; VOULGARAKIS, G.; HATAYAMA, A. et al.; Experimental investigation of plasma impedance in Linac4 H- source, **AIP Conf. Proc.** **1869**, 2017, 030038.
- [18] CASTRO, G.; BRIEFI, S.; FANTZ, U.; MASCALI, D.; MAZZAGLIA, M.; MIRACOLI, R.; NASELLI, E.; REITANO, R.; TORRISI, G.; GAMMINO, S.; Multi-diagnostics investigation of an ECR plasma confined in a simple mirror trap, 2018.
- [19] The Plone Foundation, Plone CMS: Open Source Content Management, <https://plone.org/>.
- [20] JOHNSON, L.C.; HINNOV, E.; Ionization, recombination, and population of excited levels in hydrogen plasmas, **J. Quant. Spectrosc. Radiat. Transfer** **13**, 1973, 333.
- [21] SAWADA, K.; ERIGUCHI, K.; FUJIMOTO, T.; Hydrogen-atom spectroscopy of the ionizing plasma containing molecular hydrogen: Line intensities and ionization rate, **J. Appl. Phys.** **73**, 1993, 8122.
- [22] H. P. Summers, ADAS - Atomic Data and Analysis Structure, <http://adas.phys.strath.ac.uk>.
- [23] DRAWIN, H.W.; EMARD, F.; Collisional-radiative volume recombination and ionization coefficients for quasi-stationary helium plasmas, **Z. Physik** **243**, 1971,
- [24] FUJIMOTO, T.; A collisional-radiative model for helium and its application to a discharge plasma, **J. Quant. Spectrosc. Radiat. Transfer** **21**, 1979, 439.
- [25] ALVES, L.L.; GOUSSET, G.; FERREIRA, C.M.; A collisional-radiative model for microwave discharges in helium at low and intermediate pressures, **J. Phys. D** **25**, 1992, 1713.
- [26] GOTO, M.; Collisional-radiative model for neutral helium in plasma revisited, **J. Quant. Spectrosc. Radiat. Transfer** **76**, 2003, 331.

- [27] SAWADA, K.; YAMADA, Y.; MIYACHIKA, T.; EZUMI, N.; IWAMAE, A.; GOTO, M.; Collisional-Radiative Model for Spectroscopic Diagnostic of Optically Thick Helium Plasma, **Plasma Fusion Res.** **5**, 2010, 1.
- [28] SAWADA, K.; FUJIMOTO, T.; Effective ionization and dissociation rate coefficients of molecular hydrogen in plasma, **J. Appl. Phys.** **78**, 1995, 2913.
- [29] HISKES, J.R.; Molecular Rydberg states in hydrogen negative ion discharges, **Appl. Phys. Lett.** **69**, 1996, 755.
- [30] HASSOUNI, K.; GICQUEL, A.; CAPITELLI, M.; LOUREIRO, J.; Chemical kinetics and energy transfer in moderate pressure H₂ plasmas used in diamond MPACVD processes, **Plasma Sources Sci. Technol.** **8**, 1999, 494.
- [31] GREENLAND, P.T.; Collisional-radiative models with molecules, **Proc. R. Soc. Lond. A** **457**, 2001, 1821.
- [32] SAWADA, K.; GOTO, M.; Rovibrationally Resolved Time-Dependent Collisional-Radiative Model of Molecular Hydrogen and Its Application to a Fusion Detached Plasma, **Atoms** **4**, 2016, 29.
- [33] DE HEER, F.J., Critically Assessed Electron-Impact Excitation Cross Sections for He (11S), INDC(NDS)-385, Vienna, 1998.
- [34] RALCHENKO, Yu.V., JANEV, R.K., KATO, T., FURSA, D.V., BRAY, I., DE HEER, F.J., Cross Section Database for Collision Processes of Helium Atom with Charged Particles. I. Electron Impact Processes, NIFS-DATA-59, Toki, 2000.
- [35] DRAKE, G.W. F.; High Precision Calculations for Helium, in *Springer Handbook of Atomic, Molecular, and Optical Physics*, Springer, New York, 2006, 199.
- [36] FOWLER, R.H.; Statistical equilibrium with special reference to the mechanism of ionization by electronic impacts, **Philos. Mag.** **47**, 1924, 257.
- [37] SMIRNOV, B.M., Reference Data on Atomic Physics and Atomic Processes, Springer, Berlin, 2008.
- [38] JANEV, R.K.; Atomic and Plasma-Material Interaction Data for Fusion, **Suppl. Nucl. Fusion** **4**, 1993, 1.
- [39] JANEV, R.K., REITER, D., SAMM, U., Collision Processes in Low-Temperature Hydrogen Plasmas, JÜL-4105, Jülich, 2003.
- [40] KULANDER; K. C.; GUEST, M.F.; Excited electronic states of H₃ and their role in the dissociative recombination of H₃⁺, **J. Phys. B** **12**, 1979, L501.

- [41] DATZ, S.; SUNDSTROM, G.; BIEDERMANN, C.; BROSTROM, L.; DANARED, H.; MANNERVIK, S.; MOWAT, J.R.; LARSSON, M.; Branching Processes in the Dissociative Recombination of H₃⁺, **Phys. Rev. Lett.** **74**, 1995, 896.
- [42] EERDEN, M.J. J.; VAN DE SANDEN, M. C. M.; OTORBAEV, D.K.; SCHRAM, D.C.; Cross section for the mutual neutralization reaction H₂+H⁻, calculated in a multiple-crossing Landau-Zener approximation, **Phys. Rev. A** **51**, 1995, 3362.
- [43] JOHNSON, L.C.; Approximations for Collisional and Radiative Transition Rates in Atomic Hydrogen, **Astrophys. J.** **174**, 1972, 227.
- [44] NIST, Atomic Spectra Database, www.nist.gov/pml/atomic-spectra-database.
- [45] MILES, W.T.; THOMPSON, R.; GREEN, A.E.S.; Electron-Impact Cross Sections and Energy Deposition in Molecular Hydrogen, **J. Appl. Phys.** **43**, 1972, 678.
- [46] GRZYNSKI, M.; Classical Theory of Atomic Collisions. I. Theory of Inelastic Collisions, **Phys. Rev.** **138**, 1965, A336.
- [47] BAUER, E.; BARTKY, C. D.; Calculation of Inelastic Electron-Molecule Collision Cross Sections by Classical Methods, **J. Chem. Phys.** **43**, 1965, 2466.
- [48] WEDDING, A.B.; PHELPS, A.V.; Quenching and excitation transfer for the c 3Π-u and a 3Σ+g states of H₂ in collisions with H₂, **J. Chem. Phys.** **89**, 1988, 2965.
- [49] DATSKOS, P.G.; PINNADUWAGE, L.A.; KIELKOPF, J.F.; Photophysical and electron attachment properties of ArF-excimer-laser irradiated H₂, **Phys. Rev. A** **55**, 1997, 4131.
- [50] JANEV, R.K., Private communication, 2004.
- [51] BEHRINGER, K.; FANTZ, U.; Some Basic Physics Results for Plasma Spectroscopy and Modelling, **Contrib. Plasma. Phys.** **39**, 1999, 411.
- [52] HEINEMANN, B.; FANTZ, U.; KRAUS, W.; SCHIESKO, L.; WIMMER, C.; WÜNDERLICH, D.; BONOMO, F.; FRÖSCHLE, M.; NOCENTINI, R.; RIEDL, R.; Towards large and powerful radio frequency driven negative ion sources for fusion, **New J. Phys.** **19**, 2017, 015001.
- [53] TOIGO, V.; PIOVAN, R.; BELLO, S.; DAL, G.; GAIO, E.; LUCHETTA, A.; PASQUALOTTO, R.; ZACCARIA, P.; BIGI, M.; CHITARIN, G.; MARCUZZI, D. et al.; The PRIMA Test Facility: SPIDER and MITICA test-beds for ITER neutral beam injectors, **New J. Phys.** **19**, 2017, 085004.
- [54] BACAL, M.; WADA, M.; Negative hydrogen ion production mechanisms, **Appl. Phys. Rev.** **2015**, 021305.

- [55] WÜNDERLICH, D.; SCHIESKO, L.; MCNEELY, P.; FANTZ, U.; FRANZEN, P.; THE NNBI-TEAM; On the proton flux towards the plasma grid in a RF-driven negative hydrogen ion source for ITER NBI, **Plasma Phys. Control. Fusion** **54**, 2012, 125002.
- [56] MCNEELY, P.; DUDIN, S.V.; CHRIST-KOCH, S.; FANTZ, U.; NNBI-TEAM; A Langmuir probe system for high power RF-driven negative ion sources on high potential, **Plasma Sources Sci. Technol.** **18**, 2009, 014011.
- [57] FANTZ, U.; SCHIESKO, L.; WÜNDERLICH, D.; Plasma expansion across a transverse magnetic field in a negative hydrogen ion source for fusion, **Plasma Sources Sci. Technol.** **23**, 2014, 044002.
- [58] BACAL, M.; MCADAMS, R.; LEPETIT, B.; TAKEIRI, Yasuhiko; TSUMORI, Katsuyoshi; The Negative Ion Mean Free Path And Its Possible Implications, **AIP Conf. Proc.** **1390**, 2011, 13.
- [59] GUTSER, R.; WÜNDERLICH, D.; FANTZ, U.; THE NNBI-TEAM; Negative Hydrogen Ion Transport in RF-driven Ion Sources for ITER NBI, **Plasma Phys. Control. Fusion** **51**, 2009, 045005.
- [60] FANTZ, U.; SCHIESKO, L.; WÜNDERLICH, D.; THE NNBI-TEAM; A Comparison Of Hydrogen And Deuterium Plasmas In The IPP Prototype Ion Source For Fusion, **AIP Conf. Proc.** **1515**, 2013, 187.
- [61] FANTZ, U.; BONOMO, F.; FRÖSCHLE, M.; HEINEMANN, B.; HURLBATT, A.; KRAUS, W.; SCHIESKO, L.; NOCENTINI, R.; RIEDL, R.; WIMMER, C.; Advanced NBI beam characterization capabilities at the recently improved test facility BATMAN Upgrade, accepted by Fusion Eng. Des.. **Fusion Eng. Des.**
- [62] FANTZ, U.; WÜNDERLICH, D.; A novel diagnostic technique for H-(D-) densities in negative hydrogen ion sources, **New J. Phys.** **8**, 2006, 301.
- [63] FANTZ, U.; FALTER, H.D.; FRANZEN, P.; WÜNDERLICH, D.; BERGER, M.; LORENZ, A.; KRAUS, W.; MCNEELY, P.; RIEDL, R.; SPETH, E.; Spectroscopy - a powerful diagnostic tool in source development, **Nucl. Fusion** **46**, 2006, S297.
- [64] BRIEFI, S.; FANTZ, U.; Spectroscopic investigations of the ion source at BATMAN upgrade, **AIP Conf. Proc.** **2052**, 2018, 040005.
- [65] SCHULZ-VON DER GATHEN, V.; DÖBELE, H.F.; Critical comparison of emission spectroscopic determination of dissociation in hydrogen RF discharges, **Plasma Chem. Plasma P.** **16**, 1996, 461.
- [66] SCHIESKO, L.; MCNEELY, P.; FRANZEN, P.; FANTZ, U.; THE NNBI-TEAM; Magnetic field dependence of the plasma properties in a negative hydrogen ion source for fusion, **Plasma Phys. Control. Fusion** **54**, 2012, 105002.

- [67] WIMMER, C.; SCHIESKO, L.; FANTZ, U.; Investigation of the boundary layer during the transition from volume to surface dominated H(-) production at the BATMAN test facility, **Rev. Sci. Instrum.** **87**, 2016, 02B310.
- [68] BOEUF, J.P.; CLAUSTRE, J.; CHAUDHURY, B.; FUBIANI, G.; Physics of a magnetic filter for negative ion sources. II. $E \times B$ drift through the filter in a real geometry, **Phys. Plasmas** **19**, 2012, 113510.
- [69] LISHEV, S.; SCHIESKO, L.; WÜNDERLICH, D.; FANTZ, U.; Spatial distribution of the plasma parameters in the RF negative ion source prototype for fusion, **AIP Conf. Proc.** **1655**, 2015, 040010.